Compatibility of the dimensions of polymer molecular aggregates to the pore throat of a reservoir

Risu Na and V I Erofeev
School of Earth Science & Engineering, National Research Tomsk Polythetic University, Tomsk, Russia
E-mail: narisu2011@yandex.ru

Abstract. The compatibility of the dimensions of the polymer molecular aggregates and the pore throat of the reservoir were studied. The W section of Tuha oilfield was the study area and polymers produced by Daqing Refining and Chemical Company were used. The permeability limit of the polymer molecules with different molecular masses and concentrations, matching relationship between the dimension of polymer molecular aggregates and pore throat were obtained by experiments. The results of the research are important for the development and implementation of a polymer flooding technical scheme in the middle and late stages of the operation of the Tuha oilfield.

1. Introduction

In recent years, polymer flooding has become important in the development of oilfields and in optimizing and improving productivity [1]. Polymer flooding can improve oil recovery primarily by increasing the viscosity of the injected water resulting a reduction in the permeability of the water phase. Polymers with a high relative molecular mass or concentration tend to be viscose and have a low water phase permeability [2,3]. Hence, if a polymer has a higher relative molecular mass and concentration it will be more viscous and the polymer hydration molecule should go through the natural selection of pore throat structure when passing through porous media of reservoir [4]. With the increase of relative molecular weight or concentration of polymer, the size of molecular aggregates becomes larger, the injectability becomes worse, and the mechanical trapping phenomenon of polymer in the reservoir becomes more obvious [5,6]. When the dimension of molecular aggregates is larger than the rock pore throat, it is difficult for the polymer to pass through the pore throat under normal injection pressure. When an external force is applied to push the polymer through the pore throat its molecular structure is destroyed and it loses its primary function of displacement [7,8]. The selection of polymers with regards to their molecular mass and concentration is a challenge at oilfields. Studies have been conducted on the relationship between the relative molecular mass of polymers, their permeability and their oil displacement effect, however, the results did not define the matching relationship between relative molecular mass and permeability on oil displacement effect [9,10].

This paper focuses on the evaluation of a polymer produced by Daqing Refinery and Chemical Company so as to be used at the W section of Tuha Oilfield in China. The dynamic light scattering technique was used to study the dimensions of the polymer molecular aggregates in an aqueous solution. A number of core seepage experiments were conducted to determine the core permeability limit of the polymer molecules with different molecular masses and concentrations as well as taking into consideration the relationship between the median pore radius and the dimensions of the polymer

molecular aggregates. The results of the research are important for the development and implementation of a polymer flooding technical scheme in the middle and late stages of the operation of the Tuha oilfield.

2. Experiment description

2.1. Experimental materials

Polymers (Partially hydrolyzed polyacrylamide (HPAM)) produced by Daqing Refinery and Chemical Company were used. The relative molecular mass of the HPAM polymers used were $400x10^4$, $800x10^4$, $1400x10^4$ and $2100x10^4$ respectively, and the solid content of the polymers was 88%. The experimental water which was used in place of the injection water from W section of the Tuha oil field had a mass concentration of (K^++Na^+), Ca^{2+}, Mg^{2+}, Cl^-, SO_4^{2-}, HCO_3^- of 4342, 7935, 437, 20561, 1152, 1026 mg/l respectively. The total salinity of the experimental water was 35453 mg/l. Artificial columnar cores made of quartz sand and clay cemented with epoxy resin we created and used [11]. The permeability of the artificial cores was measured using a gas and cores with different permeabilities were used. The cores were made by mixing quartz sand of different grain sizes with epoxy resin and they were all the same size i.e. they had a diameter and a length of 2.5cm and 10cm, respectively. The permeability of the cores is presented in the table 1.

2.2. Instruments and equipment for experiments

The viscosity of the polymers was measured using a DV-II Brookfield Viscometer at a shear rate of 7.34 s^{-1} at 75°C and the dimensions of the polymer molecular aggregates were measured using a Malvine NanoZS90 laser particle size analyzer system. The equipment used for core flooding tests was used to determine the seepage behavior of the polymers in the reservoir. The experimental setup consisted of an advection pump, pressure sensor, core holder, hand pump and two intermediate containers and other parts. All the equipment, except the advection pump and hand pump were placed in a thermostat with the reservoir temperature of 75 °C. The schematic diagram of the experimental process is given in Figure 1.

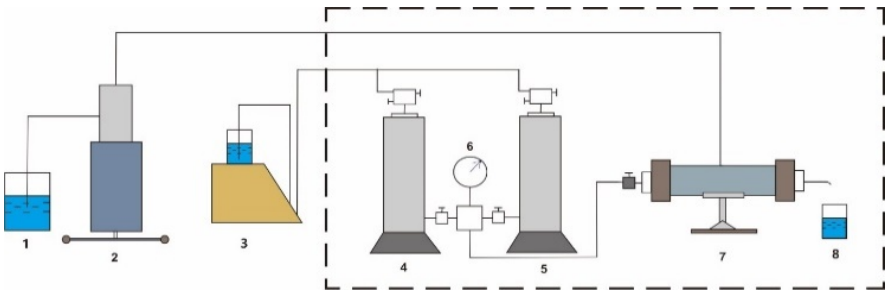

Figure 1. Experiment-process diagram: 1 – beaker, 2 – hand pump, 3 – advection pump, 4 – the container of water, 5 – the container with surfactant, 6 – sensor, 7 – core holder, 8 – measuring cup.

3. Results and discussion

3.1. Compatibility between the HPAM molecular aggregates and the pore throat

When a polymer solution passes through a core pore throat, the relationship between the injection pressure and the pore volume multiple (PV), the resistance coefficient and the residual resistance coefficient reflect its level of retention level in the porous media. It also represents its compatibility or the adaptability between polymer solution and pores of the rock. We divided the polymers into two categories based on their trends in response to the injection pressure. An increase in the injected polymer solution resulted in a stable injection pressure and was represented by a horizontal segment on the pressure curve of the seepage experiment. It showed that the polymer solution and the core pore throat were highly compatible. The lowest permeability at which the polymer solution does not plug and move through the core is called the permeability limit of the polymer solution. For the other polymer solutions

an increase in the injected polymer solution resulted in the injection pressure increasing. The increase in the injection pressure suggested that the polymer had blocked the core pores and the compatibility between the polymer and the core pore throat was low.

The seepage characteristics of the polymer solution are generally evaluated using the resistance coefficient and the residual resistance coefficient which are the technical indicators for describing the retention of polymers in porous media. The resistance coefficient (F_R) and the residual resistance coefficient (F_{RR}) were determined using the equations below [12, 13]:

$$F_R = \frac{\partial P_2}{\partial P_1} \tag{1}$$

$$F_{RR} = \frac{\partial P_3}{\partial P_1} \tag{2}$$

Table 1. Resistance coefficient (F_R) and residual resistance coefficient (F_{RR}).

M ($\times 10^4$)	C_P (mg/L)	Viscosity (mPa·s)	Permeability Kg ($\times 10^{-3}\mu m^2$)	F_R	F_{RR}
400	400	2.6	15	9.71	5.22
			20	8.03	5.13
	600	3.4	25	14.15	9.89
			30	10.59	8.25
	800	4.1	30	14.47	11.03
			35	12.33	9.74
	1000	4.8	35	15.90	11.29
			40	13.33	9.80
800	400	3.7	20	14.82	11.80
			25	10.76	8.17
	600	4.3	30	17.50	14.03
			35	13.52	9.38
	800	5.5	35	19.12	14.83
			40	13.69	11.12
	1000	6.7	40	20.53	16.12
			45	15.76	12.78
1400	400	4.2	30	19.71	15.99
			35	15.33	12.29
	600	5.8	40	23.73	17.96
			45	17.29	12.42
	800	7.9	45	24.33	20.02
			50	17.51	14.51
	1000	10.3	50	24.88	20.41
			55	17.78	13.92
2100	400	5.1	40	12.94	18.51
			45	15.96	13.33
	600	7.2	50	25.61	20.59
			55	18.76	14.54
	800	9.3	50	26.34	20.73
			60	19.44	14.65
	1000	12.4	70	29.00	22.66
			80	21.72	16.48

In the above equation, P_1 is the drop in pressure during the water flooding process, P_2 is thedrop in pressure during the chemical flooding process and P_3 is the drop in pressure during subsequent water flooding.

Experiments were conducted on the seepage characteristics of the polymer solutions using the experimental setup given in Figure 1, using polymers with different relative molecular masses (M) and polymer concentrations (Cp) to determine the permeability limit of the HPAM solution. The injection speed of the experiment was 0.3 mL/min and the pressure were measured every 30 minutes. The resistance coefficient and the residual resistance coefficient of the HPAM solution are presented in table 1. The relationship between the injection pressure of the polymer solution and the PV is given in Figure 2.

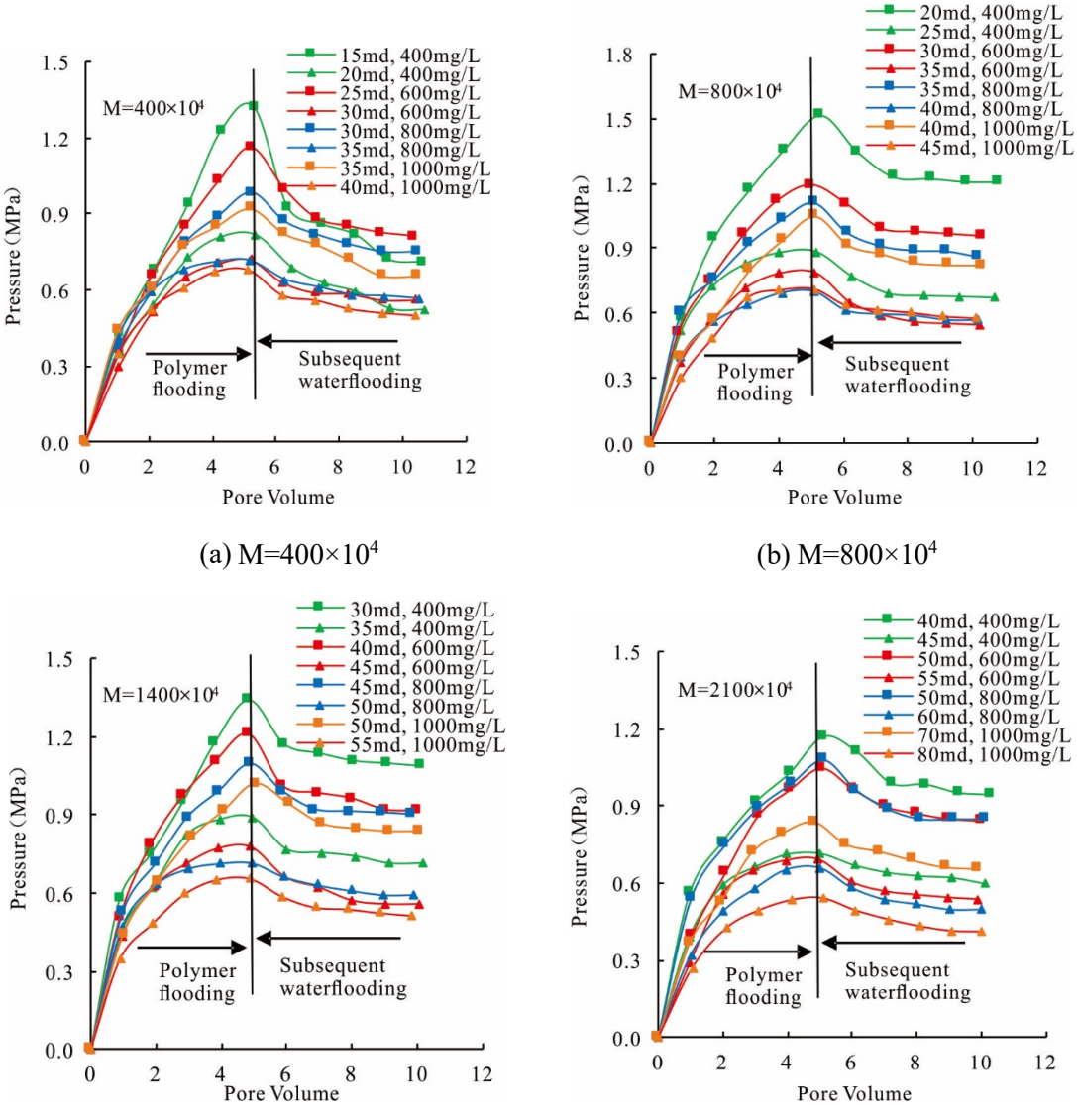

(a) M=400×10⁴ (b) M=800×10⁴

(c) M=1400×10⁴ (d) M=2100×10⁴

Figure 2. Relationship between the polymer solution injection pressure and the pore volume.

The results showed that the polymer concentration and the core permeability had a strong influence on the resistance coefficient and the residual resistance coefficient as shown in table 1. When the relative

molecular mass and the concentration of polymers were not changed, the resistance coefficient and the residual resistance coefficient of the polymer increased with a decrease in the permeability of the rock. An increase in the relative molecular mass and the concentration of the polymer solution resulted in gradual increase in the permeability limit of core. Under the same permeability conditions, the polymer solutions viscosity increased as the polymer concentration increased resulting in an increase in its resistance coefficient and residual resistance coefficient. The high residual resistance coefficient suggests that the compatibility between polymer solution and pores in the rock was high.

The dimensions of the polymer molecular aggregates were not compatible to the size of the pores of the rock when the injection pressure increased as the injection volume increased as shown in Figure 2. This is in contrast to the previous results which showed that a high compatibility resulted in a stable injection pressure as the injection volume increased as shown in Figure 2. Polymer concentration of 400 mg/L, 600 mg/L, 800 mg/L and 1000 mg/L had permeability limits of 20md, 30md, 35md and 40md, respectively, for the polymer solutions with relative molecular mass of M=400×104. The permeability limits for the polymer solutions with relative molecular mass of M=800×104 were 25md, 35md, 40md and 45md, respectively. The permeability limits of the polymer solutions with a relative molecular mass of M=1400×104 were 35md, 45md, 50md and 55md, respectively. The permeability limits of the polymer solution with a relative molecular mass of M=2100×104 were 45md, 55md, 70md and 80md, respectively.

3.2. Compatibility of the dimensions of the molecular aggregates of the polymers to the pore throat of reservoir

The dimensions of the polymer molecular aggregates (D_h) were measured using the Malvine NanoZS90 laser particle size analyzer system and the results are presented in table 2.

Table 2. D_h test results (nm)

C_p（mg/L）	Relative molecular mass（M×10^4）			
	400	800	1400	2100
400	105.5	162.5	197.3	324.7
600	130.8	187.4	242.8	378.8
800	168.3	221.3	278.3	463.5
1000	186.5	259.1	336.4	541.9

An increase in the concentration of the polymer solution resulted in an exponential increase in the dimensions of its polymer molecular aggregates. This resulted in a gradual increase in the range of D_h as the relative molecular mass of the polymer solution remained unchanged. Under a certain polymer concentration, the dimensions of the polymer molecular aggregates increased as its relative molecular mass increased, and the overall range of D_h was between 105.5 nm and 541.9 nm.

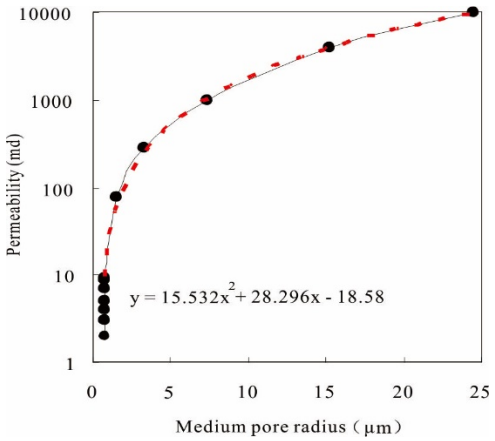

Figure 3. Relationship between the core permeability and the median pore radius.

The relationship between the reservoir rock permeability and the median pore radius (R_m) is presented in Figure 3 including the equation. The results show that an increase in the median pore radius resulted in an increase the logarithm of the permeability of the rock.

The median pore radius (R_m) of the reservoir rock corresponding to each permeability limit is presented in Figure 3. The relationship between the dimensions of the polymer molecular aggregates of the polymer solution and the median pore radius are presented in Figure 4. The relationship between the ratio of the dimensions of the polymer molecular aggregates of the polymer solution to the median pore radius (R_m/D_h) and polymer solution concentration are presented in table 3 and Figure 5.

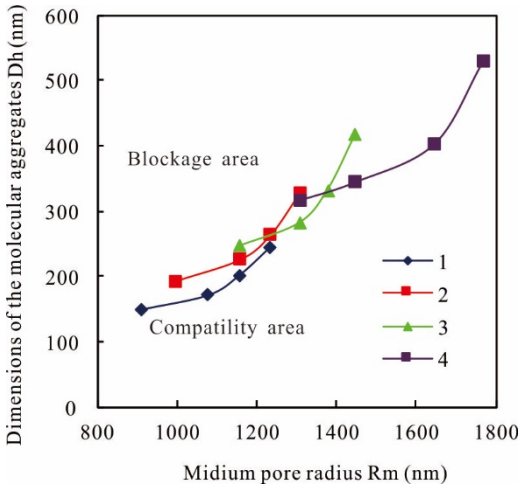

Figure 4. Relationship between the dimension of polymer molecular aggregates and the medium pore throat radius, 1 –400×10^4, 2 - 800×10^4, 3 - 1400×10^4, 4 - 2100×10^4.

The corresponding equation of line 1–3 and 4 of Figure 4 are shown in (3), (4), (5) and (6) respectively:

$$y=1\times10^{-7}x^3+0.0007x^2-1.6171x+937.11 \quad (3)$$

$$y=4\times10^{-6}x^3-0.0125x^2+13.049x-4381.2 \quad (4)$$

$$y=5\times10^{-6}x^3+0.0174x^2+19.987x-7423.4 \quad (5)$$

$$y=4\times10^{-6}x^3+0.0189x^2+27.506x-13027 \quad (6)$$

Table 3. Relationship between R_m/D_h, relative molecular mass and concentration of the polymer

C_p（mg/L）	Relative molecular mass（M×10⁴）			
	400	800	1400	2100
400	6.14	6.31	5.73	5.05
600	5.17	5.14	4.70	4.01
800	4.72	4.66	4.16	3.48
1000	4.13	4.20	4.09	3.35

The area with coordinates is divided into two parts i.e. the compatibility area and blockage area as shown in Figure 4 and Figure 5. In summary, the compatibility between the polymer and reservoir rock is determined by the permeability of the relative molecular weight and concentration of the polymer solution. An increase in the concentration of the polymer solution resulted in a gradual decrease in the ratio R_m/D_h for polymers with the same molecular weight and it ranged between 3.35 and 6.14. The cumulative percentage of the injected reservoir thickness and its corresponding reservoir permeability can be determined based on the status of the oilfield field. The injectable D_h and R_m/D_h can be determined using the corresponding equation obtained. These data have important reference value for field production.

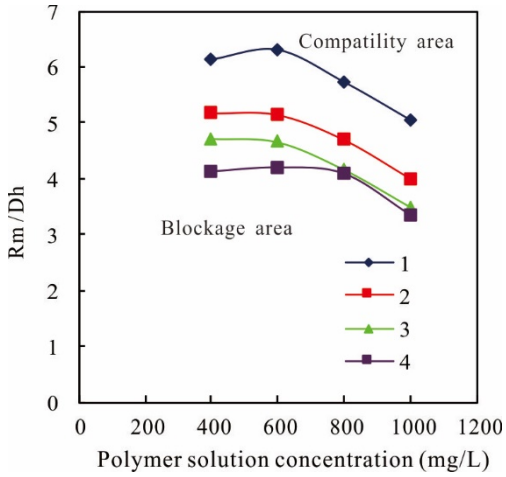

Figure 5. Relationship between R_m/D_h and the concentration of the polymers: 1 – 400×10⁴, 2 – 800×10⁴, 3 – 1400×10⁴, 4 –- 2100×10⁴.

The corresponding equation of line 1,2,3 and 4 of Figure 5 are shown in (7), (8), (9) and (10) respectively:

$$y=1\times10^{-8}x^3-3\times10^{-5}x^2+0.0244x+0.9177 \quad (7)$$

$$y=-4\times10^{-6}x^2+0.0038x+4.3114 \quad (8)$$

$$y=5\times10^{-9}x^3+1\times10^{-5}x^2+0.0106x+2.5212 \quad (9)$$

$$y=-9\times10^{-9}x^3+1\times10^{-5}x^2-0.007x+5.216 \quad (10)$$

4. Conclusion

The polymers used had concentrations of 400 mg/L, 600 mg/L, 800 mg/L and 1000 mg/L although they had different relative molecular masses. The permeability limits of the polymer solutions with a relative molecular mass of M=400×10⁴ were 20md, 30md, 35md and 40md, respectively. The permeability limits of the polymer solutions with a relative molecular mass of M=800×10⁴ were 25md,35md,40md and 45md, respectively. The permeability limits of the polymer solutions with a relative molecular mass of M=1400×10⁴ were 35md, 45md, 50md and 55md, respectively. The permeability limits of the

polymer solutions with a relative molecular mass of M=2100×10^4 were 45md, 55md, 70md and 80md, respectively. An increase in the polymer concentration resulted in a gradual decrease in the ratio R_m/D_h for the polymer solutions with the same molecular weight and it range between 3.35 and 6.14.

Acknowledgment
The work was financially supported by China National Found for studying abroad.

References
[1] Standnes D C, Skievrak I 2014 *J. Pet. Sci. Eng*. **122** 761–775
[2] Algharaib M, Alajmi A, Gharbi R 2014 *J. Pet. Sci. Eng*. **115** 17–23
[3] Erofeev V I, Lv J, Wang W 2019 *Bull. Tomsk Polytechnic University. Geo Assets Eng.* **330** 147–157
[4] Jiang W, Zhang J, Tang X 2012 *Oilfield Chem.* **29** 446–451
[5] Lu X, Zhou Y, Sun Z, Xie K, Yang H, Zhang J 2015 *Pet. Geol. Oilfield Dev Daqing* **34** 88–94
[6] Lu X, Wang X, Wang R, Wang H, Zhang S 2011 *Pet. Explor Dev* **38** 576–582
[7] Jiang X, Wang R, Lu X, Deng Q, Xiao L 2014 *Oilfield Chem* **31** 269–273
[8] Xie K, Lu X, Pan H, Han D, Hu G, Zhang J, Zhang B, Cao B 2018 *SPE Prod. Oper* **33** 1–11
[9] Narisu, Erofeev V I, Lu X, Lv J, Wang X, Zhang L 2019 *Bull. Tomsk Polytechnic University. Geo Assets Eng* **330** 136–145
[10] Xie K, Lu X, Li Q, Jiang W, Yu Q 2016 *SPE J* **21** 1–9
[11] Lu X, Gao Z, Yan W 1994 *Pet. Geol. Oilfield Dev. Daqing* **13** 53–55
[12] Liu J, Lu X, Zhou Y, Hu S, Xue B 2014 *J. China Univ.Pet* **38** 171–179
[13] Narisu, Erofeev V I, Lu X, Tian Z, Zhang L 2019 *Bull. Tomsk Polytechnic University. Geo Assets Eng.* **330** 59–68